STEREO SIDE-LOOKING RADAR EXPERIMENTS

F. LEBERL, J. RAGGAM
Technical University and Graz Research Center, A-8010 Graz, Austria

and

M. KOBRICK
Jet Propulsion Laboratory, Pasadena, California 91103, USA

ABSTRACT

The application of side-looking radar images in geoscience fields can be enhanced when using overlapping image strips that are viewed in stereo. A current question concerns the quality of stereo-radar. This paper is an attempt to describe this quality, evaluating stereo viewability and using the concept of vertical exaggeration with sets of actual radar images. A conclusion is that currently available stereo radar data are not optimized, that therefore a better quality can be achieved if data acquisition is appropriately arranged, and that the actual limitations of stereo radar are still unexplored.

Keywords: Radargrammetry, Stereo, Side-looking radar, Cartographic mapping.

1. INTRODUCTION

Stereo viewing of overlapping images is a valuable tool in photo-interpretation. It is also an indispensable technique to identify homologue image points for measurement of image coordinates and reconstruction of the three dimensional terrain. This may serve to create a model of terrain topography such as in the form of contours, or to selectively measure slopes and relative height differences.

S t e r e o refers to a visual preception of an overlapping image pair by an observer. A three-dimensional model is formed in the observer's brain. Also the computational process of generating 3-dimensional object space coordinates from sets of monocular image measurements is sometimes denoted by stereo.

For the observer radar stereo is not different from its photographic equivalent. However, there is an entirely different projection geometry and mathematical model. The human operator perceives relief displacement in the form of so-called parallax differences, just as is the case in natural binocular vision and by presentation of two images to the eyes that is called stereoscopic viewing.

There is a considerable body of literature on stereo perception. A recent review is by LaPrade et al. (1980). On radar stereo, work has been done since 1963, starting with LaPrade (1963). Most recently some numerical results were presented by Leberl (1979 a). Stereo viewability of radar images was discussed by LaPrade (1970), Graham (1975), Leberl (1975, 1978, 1979). Computational stereo was analysed by Innes (1964), Rosenfield (1968), Gracie et al. (1970), Konecny (1972), DBA-Systems (1964), Goodyear (1974), Derenyi (1975), Leberl (1972, 1975, 1978).

Commonly discussed stereo imaging arrangements have been either with both flights to the same side or each flight at opposite sides of the object. Other arrangements have been described but did not materialize, such as cross-wise flights, different flight altitudes or single flight convergent schemes such as with tilted real antennas (Leberl, 1972; Carlson, 1973; Bair and Carlson, 1974, 1975). A single flight line attempt to generate stereo SAR would fail. This has been explained in detail in a previous report (Leberl, 1979).

The current paper is an attempt at expanding previous theoretical error analyses using some real images and to evaluate them with the concept of exaggeration factors. These images are from X-band SAR (Goodyear), L-band SAR (JPL), Apollo 17 -VHF lunar imagery, SEASAT-SAR and real aperture Motorola radar. Some examples of overlapping radar images are presented; not all can be viewed sucessfully in stereo. However, a clear conclusion can not be obtained on the limiting cases where stereo is still feasible. More data are needed for that purpose.

2. STEREO GEOMETRY

2.1 General

Measurements in overlapping images schould always be made in stereo. The minimum retinal disparity for binocular vision to the observable is 3" to 20". The optimum can be achieved with lines in object space that run parallel. Monocularly two objects can be distinguished if they create an angular disparity in one eye of about 60". It is thus clear that stereo has a distinct advantage: if we were to monocularly measure the same point in two images, a measuring error will be commited in excess of 60".

2.2 Stereo Evaluation with an Exaggeration Factor

LaPrade (1970), and LaPrade et al. (1980) describe a concept for the evaluation of stereo viewability and quality using a vertical exaggeration factor, q. This is related to central perspective geometry which in turn is the model used to explain human vision. For ease of reference we present this concept of LaPrade. Figure 1 describes an observer looking at a stereoscopic image pair through the lenses of a stereoscope, the central perspective image collection geometry for a pair of cameras and both illustrated for a pyramid-shaped object. The exaggeration factor that is of relevance results from the ratio h/w of the pyramid as it is

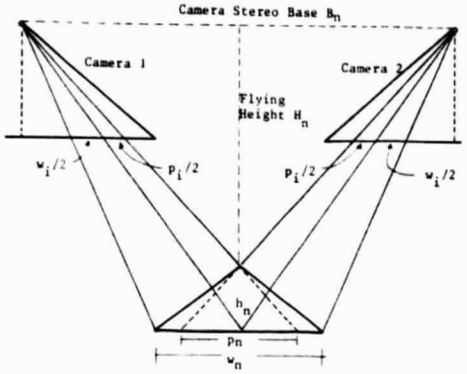

Figure 1a: Definitions in object space for the vertical exaggeration factor after LaPrade et al. (1980).

in object space (h_n/w_n) and as it appears from the stereo observations, h_s/w_s. This is thus a measure of the f l a t n e s s of the subjectively observed stereo model.

In addition to the ratio in nature, h_n/w_n, and in the stereo-observation, h_s/w_s, there is a corresponding ratio in image, dp_i/w_i according to Figure 1b.

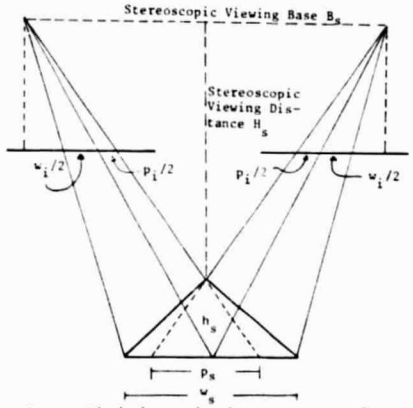

Figure 1b: Definitions in image space for vertical exaggeration

This ratio also exists in the object reference plane dp_n/w_n. We find

$$dp_n/w_n = dp_i/w_i \quad (1)$$

$$dp_n/h_n = B_n/H_n \quad (2)$$

B_n is the equivalent camera stereo base and H_n the equivalent camera flying heigh. Thus:

$$dp_i/w_i = (B_n/d_n)\, h_n/w_n \quad (3)$$

The stereoscopic observation has a stereo base, B_s and distance to the virtual image, H_s. We find again from Figure 1:

$$h_s/dp_s = H_s/B_s \quad (4)$$

$$dp_s/w_s = dp_i/w_i$$

Thus

$$h_s/w_s = (H_s/B_s)\,(dp_i/w_i)$$

and

$$h_s/w_s = (H_s/B_s)(B_n/H_n)(h_n/w_n) \quad (5)$$

The vertical exaggeration, q, is then:

$$q = (h_s/w_s)/(h_n/w_n) \quad (6)$$

This is, for equivalent central perspective imaging:

$$q = (H_s/B_s)(B_n/H_n) \quad (7)$$

According to LaPrade et al. (1980) optimum stereo viewing with a stereoscope requires the ratio

$$H_s/B_s \approx 5$$

This will be applied to radar images.

3. RADAR STEREO

3.1 Viewability

The two partners of a stereo image pair must be very similar in image quality or thematic content (tone, texture, etc.) so that they correlate well, whereas they should be sufficiently different in geometry to present parallaxes for height perception.

Radar is actively illuminating the object. Differences in geometry due to different sensor positions therefore imply also illumination differences.

From a geometric point of view good stereo contradicts with good viewability. In aerial photo interpretation the required parallaxes are obtained without any illumination differences in the two stereopartners: the sun illumination hardly changes from one photograph to the next. Stereo viewability is not a problem with photography. It is the essential problem with **radar**. Figures 2 through 8 present some examples of stereo radar models from:

(i) aircraft at shallow look angles, with same-side illumination (Figures 3, 4);
(ii) aircraft at shallow look angles, with opposite side illumination (Figure 2);
(iii) aircraft with same-side illumination and satellite SAR (Figures 4 and 5);
(iv) satellite (SEASAT) with same-side and opposite-side illumination (Figures 6 and 7);
(v) lunar Apollo 17 radar with same-side illumination (Figure 8).

Figure 2: Opposite-side stereo with aircraft radar (Courtesy Goodyear - Aeroservice), 3 cm wavelength. Estrella Mts. / Arizona.

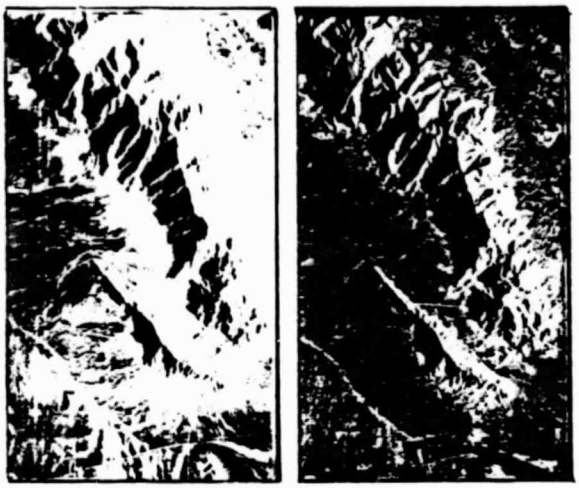

Figure 3: Same-side stereo with aircraft radar (Courtesy Goodyear - Aeroservice); Estrella Mountains / Arizona, flying height 12 km, 3 cm wavelength.

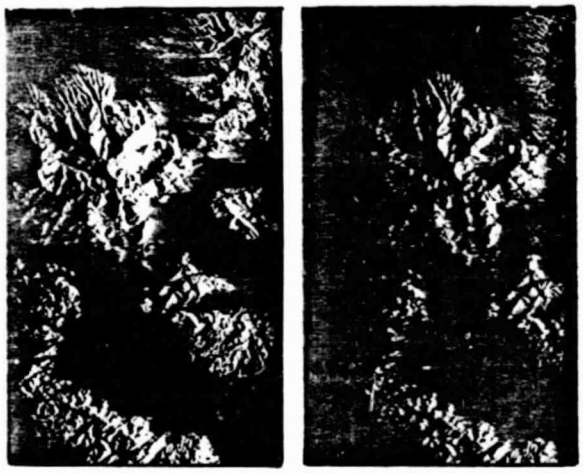

Figure 4: Same-side stereo with aircraft radar Granite Mountain, Arizona, 12 km altitude, (Courtesy Goodyear - Aeroservice);

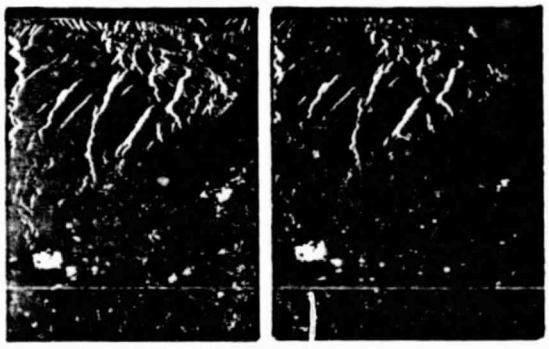

Figure 6: SEASAT-SAR same-side stereo of Los-Angeles

Figure 5: Same area as Fig. 4, SEASAT-SAR, 800 km altitude, 25 cm wavelength.

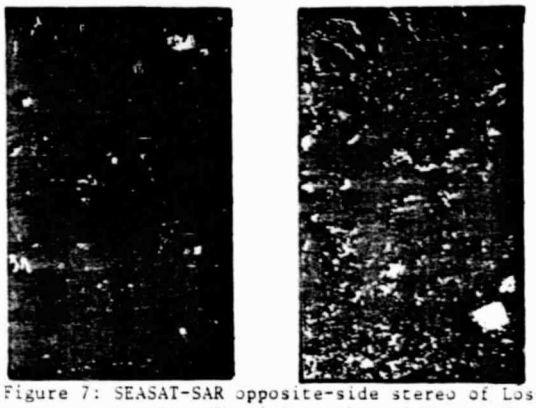

Figure 7: SEASAT-SAR opposite-side stereo of Los-Angeles. Partial overlap with area in Fig.6

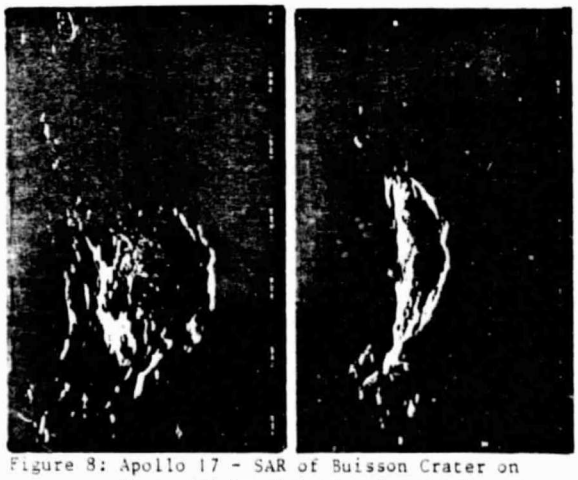

Figure 8: Apollo 17 - SAR of Buisson Crater on Moon, 116 km altitude, 2 m wavelength.

Table 1 reviews a set of stereo configurations, including those shown here, with a subjective evaluation of viewability by an observer. The conclusion from the study of a larger set of radar stereo pairs confirms earlier findings (Leberl, 1979). Influencing factors on stereo are:

stereo arrangement;
look-angles off-nadir;

stereo intersection angles;
ruggedness of the imaged area.

Type of Radar	Number of Models Studied	Base Length (km)	Look Angles Ω'	Type of Stereo	Intersection Angle ΔΩ	Type of Terrain	Stereo Viewability
SEASAT	10	25 - 75	20°	Same-side	1°3 - 4°8	Rugged	very convenient
SAR	1	550	20°	Opposite-side	40°	Rugged	not possible
Aircraft SAR	4	0.7 - 13	68°	Same-side	0°2 - 23°	Rugged	very convenient
Goodyear	2	30	68°	Opposite-side	120°	flat to Rugged	only when flat
Aircraft Real Aperture	1	10	81°	Same-side	6°	flat to hilly	convenient
Motorola	1	48	80°	Opposite-side	160°	flat to hilly	only when flat
Lunar Apollo 17 ALSE-SAR	19	0.7 - 10.3	10°	Same-side	0°3 - 5°3	flat	convenient
						Rugged	only with ΔΩ < 1°9

Table 1: Summary of viewability test for radar stereo with actual imagery.

Viewability is thus ensured at shallow look angles for same-side arrangements. Opposite-side stereo is feasible with flat or gently rolling terrain. The limits of the actual performance cannot be defined even with the material available today. One will have to investigate this with the help of an even larger set of images, in particular with a larger variety of cases; image simulation offers a means to evaluate the subjective capability of an observer viewing radar stereo data.

LaPrade (1975) reports on one experiment with operators studying same-side stereo of flat areas with man-made objects. Optimum results were reported to require look angles of 37° to 67° off-nadir and intersection angles of about 12° to 15°. These intersection angles may seem poor, but it will be shown later that radar has the potential to still produce vertical exaggeration factors approaching those of standard photo-interpretation.

3.2 Computations

A general formulation for radar stereo computations was reviewed by Leberl (1979) and is beyond the current context. Simplified formulations are more commonly employed. For these a recti-linear flight at constant altitude is assumed with the flight direction parallel to the object-x-coordinate axis (Figure 9). We read from the figure that the object

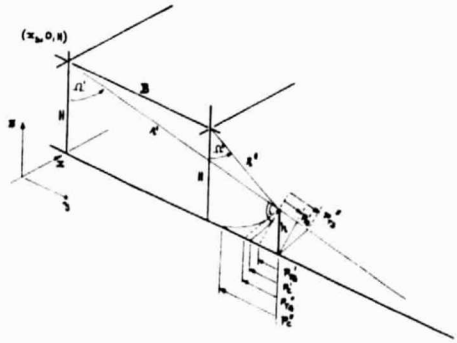

Figure 9: Geometry of stereo computation.

x_p, y_p, z_p-coordinates of a point p are:

$$\begin{aligned} x_p &= x_s \\ y_p &= (r'^2 - r''^2 + B^2)/(2B) \\ z_p &= H - (r'^2 - y_p^2)^{1/2} + (r''^2 - (B-y_p^2)^{1/2})/2 \end{aligned} \qquad (8)$$

where B is the stereo base, H is the flying height.

A slightly different approach to compute the height h above a reference datum is still with projection cercles:

$$\begin{aligned} y &= \tan\Omega' \ (H-h) \\ y &= \pm \tan\Omega'' \ (H-h) + B \\ h &= H - B/(\tan\Omega' \pm \tan\Omega'') \end{aligned} \qquad (9)$$

We need to relate to object height h above a reference datum to parallax differences dp measured in an image pair. We read directly from Figure 9, replacing the actual projection cercle by a tangent at the object point:

$$\begin{aligned} p'_{TG} &= h \ \cot\Omega' \\ p''_{TG} &= h \ \cot\Omega'' \\ dp_{TG} &= p''_{TG} \pm p'_{TG} = h(\cot\Omega'' \pm \cot\Omega') \\ h &= dp_{TG} \ /(\cot\Omega'' \pm \cot\Omega'). \end{aligned} \qquad (10)$$

where the + sign applies to opposite and the - sign to same-side stereo.

An object height h can be computed if in addition to the parallax difference dp one also knows the look angles Ω', Ω''. Clearly a given parallax difference dp generates different heights h, depending on Ω', Ω''. This is in contradiction to photographic stereo computation, where a given parallax difference relates to the same height, irrespective of where in the stereo model it has been measured.

Equ. 10 applies to ground range presentation as shown in Figure 9 . In a slant range case, an observed parallax difference needs to be converted to a height h through a different formula. We have from Figure 9:

$$\begin{aligned} dp_{TS} &= p'_{TS} - p''_{TS} \\ p'_{TS} &= h \cos\Omega' \\ p''_{TS} &= h \cos\Omega'' \\ h &= dp_{TS} \ / \ (\cos\Omega'' \pm \cos\Omega') \end{aligned} \qquad (11)$$

where + is for opposite-, - for same-side cases.

Equs. (10) and (11) are approximations since the actual projection cercles of radar are replaced by tangent lines. These approximations become increasingly coarse as look angles Ω', Ω'' reduce to smaller values. According to Figure 9, the parallax dp is more correctly related to height h as follows:

$$p'_C = y - (r'^2 - H^2)^{1/2}$$
$$p''_C = y - B - (r''^2 - H^2)^{1/2}$$
$$dp_C = B + (r''^2 - H^2)^{1/2} - (r'^2 - H^2)^{1/2} \quad \ldots \quad (12)$$

This is a non-linear relationship between dp_C and h, where h is included in r', r'':

$$dp_C = B + ((H - h)^2 / \cos^2\Omega'' - H^2)^{1/2}) - ((H - h)^2 / \cos^2\Omega'' - H^2)^{1/2} \quad (13)$$

This expression will be used to compute the exaggeration factors of radar stereo.

4. DEFINITION OF RADAR STEREO EXAGGERATION

The exaggeration factor q, as defined for camera photography relates a subjectively observed pyramid in the stereo model to the same pyramid in object space. Since we can relate the radar stereoparallax dp to an equivalent photographic stereo case it is possible to compare the quality of a radar stereo model with camera stereo. We need to find the photographic base-to-height ratio, B_n/H_n, of a fictitious camera that would produce a parallax dp for a given object height h. The exaggeration factor q, is:

$$q \approx 5\ B_n / H_n \quad (14)$$

But B_n/H_n is in turn, in the case of a camera

$$B_n / H_n = dp_n / h_n$$

Therefore

$$q \approx 5\ dp_n/h_n$$

The ratio dp/h needs to be related to radar. Using Equs. (10) and (11) we obtain a value q':

$$q' \approx 5\ (\cos\Omega'' \pm \cos\Omega')$$

or

$$q' \approx 5\ (\cot\Omega'' \pm \cot\Omega')$$

for slant- and ground-range presentations, respectively.

But for small angles Ω', Ω'' such as those in satellite radar, these equations represent merely an approximation. It would thus be appropriate to employ equ. (13) to avoid neglections due to approximations.

Table 2 presents the computed values of dp for various stereo cases and the corresponding exaggeration factor q as obtained with equ. (13) for dp_C/h. to effects of neglections, Table 2 also contains the values of q'.

We see that the exaggeration factors and thus the stereo parallaxes that are obtained with radar in a ground range presentation, can compare well with photographic stereo: as look angles become steeper, one has a more accentuated stereo-effect in spite of small stereointersection angles. The effect assumes extreme values for a case such as Apollo 17-ALSE, where very small intersection angles create parallaxes that are multiples of the object height. In camera photogrammetry, the largest parallaxes are of the order of an observed height difference, and q-values amount to 3 - 5.

It must be emphasised that the exaggeration factor is not a promise of high accuracy: for radar it can well be that errors propagate strongly into parallaxes and are magnified with the parallaxes themselves.

An interesting fact is the difference of observed parallaxes in slant and ground range presentation: in the latter the parallax differences are magnified particularly with steep look angles.

5. ACCURACIES WITH PARALLAX MEASUREMENTS

Several stereo models were used to take parallax measurements in two ways: with a stereoscope and parallax bar, and with a conventional photogrammetric plotter used as a comparator. All images are of the same-side type.

The measurements were taken in 6 stereo models and height differences dh were computed between known heights h and radargrammetrically determined ones. These discrepancies were used to define a correction polynomial:

$$z = \sum_{i=1}^{I+1} \sum_{j=1}^{J+1} \sum_{k=1}^{K+1} a_{ijk}\, x^{i-1}\, y^{j-1}\, z^{k-1} \quad (15)$$

Table 3 presents the results of this exercise in the form of root mean square residuals. The stereoplotter was not superior to simple parallax bar measurements.

In Table 3 there were 6 stereo cases incasured with both aircraft and satellite radar. These are denoted in the Table with numbers I through IV. Also the polynomial was used with various choices of coefficience.

The stereo model cases used are as follows:

I ... Granite Mountain, satellite, parallax bar

II... Granite Mountain, satellite, stereoplotter

Type of Radar	Stereo Base km	Look Angle Ω' (°)	Intersection Angle $\Delta\Omega'$ (°)	Flying Height H (km)	Parallax Diff. due to h= 1km Ground ranges	Exaggeration Factors If Ground Ranges		If Slant Ranges	
						Rigourous q	Approximate q'	q	q'
SEASAT	25	20°	1°.6	800	0.263	1.3	1.3	0.05	0.05
	75	22°	4°.8	800	0.761	3.8	3.8	0.14	0.14
Aircraft SAR Goodyear	0.7	68°	0°.5	12	0.011	0.06	0.05	0.04	0.04
	13.5	65°	23°	12	0.720	3.6	3.2	1.60	1.60
Aircraft RAR Motorola	10	81°	10°	4	0.215	1.1	0.9	0.95	0.85
	48	80°	160°	4	0.414	2.1	1.8	2.01	1.74
Apollo 17 ALSE Moon	0.7	10°	0°.3	115	0.383	1.9	0.9	0.00	0.00
	3.9	10°	1°.9	116	3.422	17.1	6.8	0.03	0.03
	10.0	13°	4°.7	116	2.584	12.9	6.4	0.07	0.07
	10.0	13°	4°.8	116	5.220	26.1	10.6	0.08	0.08

Table 2: Exaggeration factors for radar stereo models, all related to ground range representations.

The values of q' due to equs. (10) or (11) can be different from q. To quantify these differences due

III... Granite Mountain, aircraft, parallax bar

IV ... Granite Mountain, aircraft, stereoplotter

V ... Los Angeles, optically corr., parallax bar

VI ... Los Angeles, digitally corr., parallax bar

Table 3: Accuracies of stereo-radar-derived heights.

Polynomial	Number of Polynomials coefficients	I	II	III	IV	V	VI
1 2 3		20 points	21 points	21 points	21 points	20 points	20 points
1 - 1 - 0	4	350	352	365	365	474	430
2 - 2 - 2	17	98	121	49	48	143	121
1 - 1 - 1	8	140	139	138	134	274	202
2 - 1 - 1	11	135	130	78	106	199	230
1 - 2 - 1	11	121	134	133	128	256	207
1 - 1 - 2	11	136	124	124	120	217	218
1 - 2 - 2	14	99	122	99	70	180	161

There are considerable systematic errors in all raw heights that need to be corrected with the use of control points and correction polynomials. Aircraft radar provided higher accuracies than SEASAT, althoug the differences are not distinct with lower order correction functions.

Satellite radar of Los Angeles is poorer than of Granite Mountain because of a smaller stereo base. Digital and optical correlations led to the same performance figures.

6. CONCLUSIONS

An evaluation with a large set of about 40 radar stereo models demonstrates that same-side arrangements provide good stereo viewability; this was confirmed for aircraft radar with look angles off-nadir of 60° to 80° and intersection angles between 0.2° and 23°, and for satellite radar (SEASAT) with look angles of 20° and intersection angles of 1.2° to 4.8°. In the case of extremely steep illumination such as in the Apollo 17 ALSE-radar on the Moon, same-side stereo of mountainous areas was impossible when the intersection angles were in excess of about 2°. Look angles were around 10° in that project. No other radar stereo was available. Its viewability at other look- and intersection angles remains thus unexplored.

Height accuracies in same-side aircraft radar of mountainous terrain amounted to + 150 m after an 8 parameter polynomial correction. Satellite radar from SEASAT was somewhat inferior with errors in excess of + 200 m for the same areas and same type of correction polynomial. Again this concerns currently available stereo cases with their inherent limitations.

Vertical exaggeration factors were between 0.06 and 3.6 for aircraft, between 1.3 and 3.8 for SEASAT and between 1.9 and 26 for Apollo 17 data. This compares with a value of q = 3 to 5 for standard aircraft wide-angle photography. We see for the very small intersection angles of satellite radar that the vertical exaggeration factors are rather large. This, however, is valid due to the small look angles off-nadir where small intersection angles still create large parallaxes in ground range presentations. The large exaggeration factors are not existent in slant range presentations.

For more complete evaluation of the effect of radar stereo arrangements on viewability, accuracy and exaggeration factors, one would need a more complete set of images covering a wider range of parameters. A potentially usetul approach is through image simulation.

This may be helpful in exploring more fully the actual limitations of stereo radar for visual inspection and interpretation of a given terrain.

ACKNOWLEDGEMENT

The cooperation of M. Kobrick in this project is due to one phase of research performed at the JET PROPULSION LABORATORY, through NASA contract NAS 7-100. The participation of the other authors was possible due to research contract No. 6.931/3-27/1980 by the Austrian Ministry of Science and Research.

REFERENCES

1. Bair G L and Carlson G E 1975, Height Measurement with Stereo Radar, *Photogramm. Eng. and Remote Sensing*, Vol. XLI.

2. Bair G L and Carlson G E 1974, Performance Comparison of Techniques for Obtaining Stereo Radar Images, *IEEE Trans. on Geoscience Electronics*, GE-11.

3. Carlson G E 1973, An Improved Single Flight Technique for Radar Stereo, *IEEE Trans. on Geoscience Electronics*, GE-11, No. 4.

4. DBA-Systems 1974, *Research Studies and Investigations for Radar Control Extensions*, DBA Systems, Inc., P.O. Drawer 550, Melbourne, Florida, Defense Documentation Center Report No. 530784L.

5. Derenyi E E 1975, Topographical Accuracy of Side Looking Radar Imagery, *Bildmessung und Luftbildwesen*, 1975, No. 1.

6. Goodyear 1974, *Preliminary Imagery Data Analysis Goodyear Electronic Mapping System (GEMS)*, Goodyear Aerospace Corp., Report GIB-9342, Code 99696.

7. Gracie G et al 1970, *Stereo Radar Analysis*, US Engineer Topographic Laboratory, Ft. Belvoir, Virginia. Report No. FTR-1339-1.

8. Graham L 1975, Flight Planning for Radar Stereo Mapping, *Proc. Am. Soc. Photogramm.*, 41 st. Meeting, Washington, D.C.

9. Innes R B 1964, *Principles of SLAR Measurements of the Third Coordinate of Target Position*, Report of Project Michigan No. 2900-474-T.

10. Konecny G 1972 , Geometrische Probleme der Fernerkundung, *Bildmessung und Luftbildwesen*, Vol. 42, No. 2.

11. LaPrade G L 1963, An Analytical and Experimental Study of Stereo for Radar, *Photogramm. Eng.*, Vol. XXIX.

12. LaPrade G L 1970, *Subjective Considerations for Stereo Radar*, Goodyear Aerospace Corp., Report GIB-9169, and Photogramm. Eng.

13. LaPrade G 1975, *Addendum to GIB-9169*, Subjective Considerations for Stereo Radar, Goodyear Aerospace Corp., Arizona Division.

14. LaPrade G et al 1980, Stereoscopy, *Manual of Photogrammetry*, 4 th Edition, American Society of Photogrammetry, Falls Church, USA.

15. Leberl F 1972, On Model Formation with Remote Sensing Imagery, *Interr. Zeitschrift für Vermessungswesen*, Vol. 60.

16. Leberl F 1975 , Lunar Pradargrammetry with ALSE-VHF-Imagery, *Proc. Am. Soc. Photogramm.*, Fall Tech. Meeting, Phoenix, Arizona.

17. Leberl F 1978, *Satellitenradargrammetrie*, Deutsche Geodätische Kommission, Series C, No. 239, Munich 156 p.

18. Leberl F 1979, *Accuracy Aspects of Stereo-Side-Looking Radar*, JPL-Publication 1979 - 17, Jet Propulsion Laboratory, Pasadena, USA.

19. Rosenfield G H 1968 , Stereo Radar Techniques, Photogramm.Eng., Vol.XXXIV.